



Mechanical properties and wear and corrosion resistance of electrodeposited Ni–Co/SiC nanocomposite coating

Lei Shi^{a,b}, Chufeng Sun^{a,b}, Ping Gao^a, Feng Zhou^a, Weimin Liu^{a,*}

^a State Key Laboratory of Solid Lubrication, Lanzhou Institute of Chemical Physics,
Chinese Academy of Sciences, Lanzhou 730000, PR China

^b Graduate School, Chinese Academy of Sciences, Beijing 100039, PR China

Received 24 March 2005; received in revised form 18 May 2005; accepted 19 May 2005

Available online 21 June 2005

Abstract

Ni–Co/SiC nanocomposite coatings with various contents of SiC nano-particulates were prepared by electrodeposition in a Ni–Co plating bath containing SiC nano-particulates to be co-deposited. The influences of the nanoparticles concentration, current density, stirring rate and temperature of the plating bath on the composition of the coatings were investigated. The shape and size of the SiC nano-particulates were observed and determined using a transmission electron microscope. The polarization behavior of the composite plating bath was examined on a PAR-273A potentiostat/galvanostat device. The wear behavior of the Ni–Co/SiC nanocomposite coatings was evaluated on a ball-on-disk UMT-2MT test rig. The worn surface morphologies of the Ni–Co/SiC nanocomposite coatings were observed using a scanning electron microscope. The corrosion behavior of the nanocomposite coatings was evaluated by charting the Tafel curves of the solution of 0.5 mol L⁻¹ NaCl at room temperature. It was found that the cathodic polarization potential of the composite electrolyte increased with increasing SiC concentration in the plating bath. The microhardness and wear and corrosion resistance of the nanocomposite coatings also increased with increasing content of the nano-SiC in the plating bath, and the morphologies of the nanocomposite coatings varied with varying SiC concentration in the plating bath as well. Moreover, the co-deposited SiC nano-particulates were uniformly distributed in the Ni–Co matrix and contributed to greatly increase the microhardness and wear resistance of the Ni–Co alloy coating.

© 2005 Elsevier B.V. All rights reserved.

Keywords: Electrodeposition; Ni–Co alloy coating; SiC nano-particulates; Nanocomposite coating; Wear behavior

1. Introduction

Ceramic or metal matrix nanocomposites containing dispersed second-phase particulates usually have various special properties such as dispersion hardening, self-lubricity, high temperature inertness, good wear and corrosion resistance, and chemical and

* Corresponding author. Tel.: +86 931 4968166;
fax: +86 931 8277088.
E-mail address: wmliu@ns.lzb.ac.cn (W. Liu).

biological compatibility [1–5]. This accounts for the increased application of Ni-based nanocomposites in automobile industry. In order to meet the requirement for developing novel ceramic- and metal-based nanocomposites, many preparation techniques have been investigated. As a technique conducted at a normal pressure and ambient temperature and of low cost and high deposition rate, electrodeposition is considered to be one of the most important techniques for producing nanocomposites and nanocrystals [6–8].

With a view to the correlation among the structures and properties of composites, it could be practicable to endow electrodeposited nickel–cobalt alloy coatings with special properties different from that of the plated alloy coating, by incorporation of second-phase ceramic nano-particulates, because the inorganic nano-particulates such as SiC, Al₂O₃, and ZrO₂ possess good chemical stability, high microhardness, and good wear resistance and corrosion resistance at elevated temperature [9–11]. Therefore, it would be rational to anticipate that electrodeposited Ni–Co/ceramic nano-particulates composite coatings have higher strength and hardness, specific magnetic properties, better chemical stability, and better wear and corrosion resistance at elevated temperature than the Ni–Co alloy coating [12–16], since the composite coatings combine the advantages of both the electrodeposited Ni–Co coating and the ceramic nano-particulates. In such a way the application fields of the Ni–Co alloy-based electrodeposited coatings as a kind of high temperature wear-resistant and anticorrosive coating would be greatly broadened to the severe environments containing water or corrosive compounds which may cause severe wear and oxide scaling at elevated temperatures. Thus it is unsurprising that the electrodeposited composite coatings consisting of alloy matrixes and dispersed nano-particulates, for example, Ni–Fe–nano-Si₃N₄ [17], Co–Ni–nano-Al₂O₃ [18], Zn–Ni–nano-SiC coatings [19], and Ni–Co–nano-Si₃N₄ [20], have been recently extensively focused on. Ni–Co alloy has been widely used as the recording head materials for computer hard drive industries. In the case of micro-electrical mechanical system (MEMS), the magnetic layer thickness can vary from a few nanometers to a few millimeter, depending on the applications. The magnetic thin films must also have good adhesion, low-stress, and good corrosion resistance, and be

thermally stable with excellent magnetic properties. The well-dispersed nano-sized SiC particles in a Ni–Co matrix can not only enhance the mechanical properties, but also would be a necessity for the use as the composite materials in microdevices. Unfortunately, most of the availed reports in this respect are focusing on the SiC powders in a size of micron, and so far no work has been reported on the preparation and performance investigation of nano-sized SiC reinforced Ni–Co composite coatings.

Thus Ni–Co/SiC nanocomposite coatings were prepared by the electrodeposition in a nickel–cobalt plating bath containing SiC nano-particulates. The microstructure and surface morphology of the composite coatings were investigated. The effects of the incorporated SiC on the mechanical properties and wear and corrosion resistance of the nanocomposite coatings were analyzed.

2. Experimental

The plating bath is composed of 200 g L⁻¹ NiSO₄, 40 g L⁻¹ NiCl₂, 40 g L⁻¹ CoSO₄, 50 g L⁻¹ Na₃C₆H₅O₇, 30 g L⁻¹ H₃BO₃, 1–20 g L⁻¹ SiC, and 5 g L⁻¹ saccharin. Analytical reagents and distilled water were used to prepare the plating solution. Prior to plating, the SiC nano-particulates of a mean diameter 50 nm (Kaier, Hefei, China) were dispersed in the electrolyte in the presence of saccharin. The electroplating tests were performed on a model 273A potentiostat/galvanostat device (EG&G Princeton Applied Research). The electrodeposition was conducted at a current density of 30 mA cm⁻². A platinum plate of 40 mm × 40 mm was used as the anode, while a saturated calomel electrode (SCE) was used as the reference electrode. A rectangular copper plate of a size 10 mm × 10 mm and a surface roughness less than 0.02 μm was used as the cathode substrate to be plated. The substrates were sequentially ultrasonically cleaned in ethanol, acetone, and distilled water for 10 min, activated in 1:1 HCl for 30 s, washed in distilled water, and then immersed immediately in the plating bath to allow the electrodeposition of the target naocomposite coatings.

The cathodic polarization curves of the electrolyte were recorded at a sweep rate of 0.1 mV/s. The Tafel curves were measured at a sweep rate of 0.01 mV/s in

0.5 mol L⁻¹ NaCl at room temperature. The morphologies of the nanocomposite coatings were observed using a scanning electron microscope (JEOL JSM-5600LV) and the composition of the nanocomposite coatings was determined using an energy dispersive spectrometer (EDS) coupled with the SEM. The phase structure of the nanocomposite coatings was analyzed on a D-max/Rb X-ray diffractometer (XRD). The shape and size of the nano-SiC were observed and determined using a transmission electron microscope (TEM, JEM2010). The hardness of the nanocomposite coatings with a thickness about 20 μm was measured on a Vickers' microhardness instrument at an applied load of 50 g for 5 s. Five measurements were conducted on each sample and the results were averaged. Since the measurement of hardness is always influenced by the substrate, we used the Jönsson and Hogmark method [21] to dissociate the contributions of the substrate and coating of measured hardness. The deviation of the average hardness is less than 5%. The tribological behaviors of the electrodeposited nanocomposite coatings reciprocally sliding against SAE52100 steel ball ($\phi 3$ mm) were examined on a UMT-2MT tribometer in a ball-on-disk configuration. The sliding was performed at an amplitude of 5 mm, a normal load of 1 N, and a frequency of 5 Hz. All the friction and wear tests were performed under unlubricated condition at room temperature and in ambient air (relative humidity 48–52%). The friction coefficient was recorded continuously during the tests.

3. Results and discussion

3.1. TEM observation of SiC nano-particulates

Fig. 1 shows the TEM image of the SiC nano-particulates (the specific surface area is reported to be 90 m² g⁻¹ by the producer). It is seen that they appear as microspheres of a diameter about 50 nm. The β -SiC nano-particulates have a density of 0.05 g cm⁻³ and a face centered cubic structure.

3.2. Polarization behavior of Ni–Co/SiC electrolyte

Fig. 2 shows the cathodic polarization curves of the Ni–Co/SiC electrolytes containing different concentra-

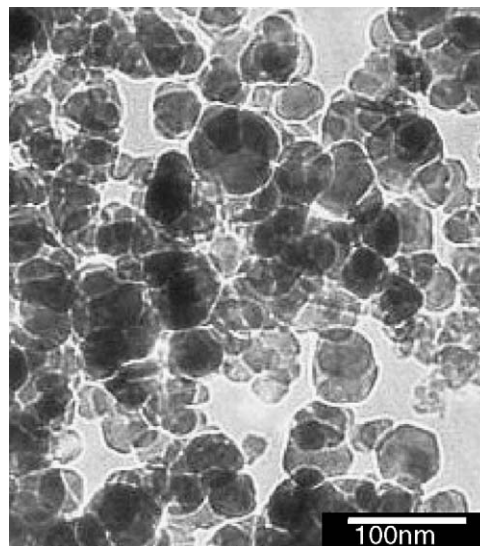


Fig. 1. TEM image of SiC nano-particulates.

tions of SiC nano-particulates. It is seen that the addition of SiC nano-particulates to the electrolyte causes the reduction potential of Ni–Co to shift towards larger negatives, but the slope of the reduction curve keeps unchanged. The shift to a lower value in the reduction potential is attributed to a decrease in the active surface area of the cathode, owing to the adsorption of the SiC particulates, and may also relate to the decrease in the ionic transport by the SiC nano-particulates, which does not significantly affect the electrochemical reaction mechanism. This observation conforms to what has been reported by Wu et al. [18].

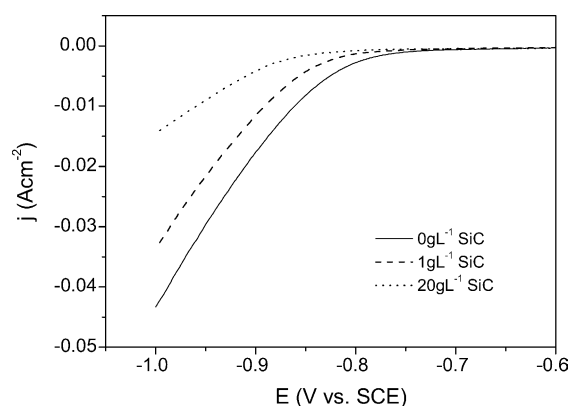


Fig. 2. Cathodic polarization curves for the co-deposition of Ni–Co/SiC at different concentrations of SiC particulates in the plating bath.

3.3. Factors affecting the composition of the composite coating

Fig. 3 shows the relationship between the weight percentage of the co-deposited SiC particulates in the coating and the concentration of the same particulates in the electrolyte. It is seen that the weight percentage of the SiC nano-particulates in the composite coating increases sharply with increasing SiC particulates content up to 5 g L^{-1} in the electrolyte. As the SiC concentration in the electrolyte surpasses 5 g L^{-1} , the weight percentage of the SiC nano-particulates in the composite coating decreases. This similar behavior is observed in other cases [1,19]. Namely, the weight percentage of the co-deposited SiC particulates reaches a maximum when the concentration of the SiC nano-particulates is kept at an optimal value of 5 g L^{-1} . The increase in the co-deposited SiC nano-particulates with increasing SiC particulates content up to 5 g L^{-1} in the electrolyte can be explained by Guglielmi's two-step adsorption model [20,21]. In other words, a higher concentration of SiC particulates in the electrolyte enhanced the adsorption rate, thus resulting in a higher weight percentage of the co-deposited SiC nano-particulates; while the decrease in the weight percentage of the co-deposited SiC nano-particulates at a concentration of SiC nano-particulates above 5 g L^{-1} is attributed to the agglomeration

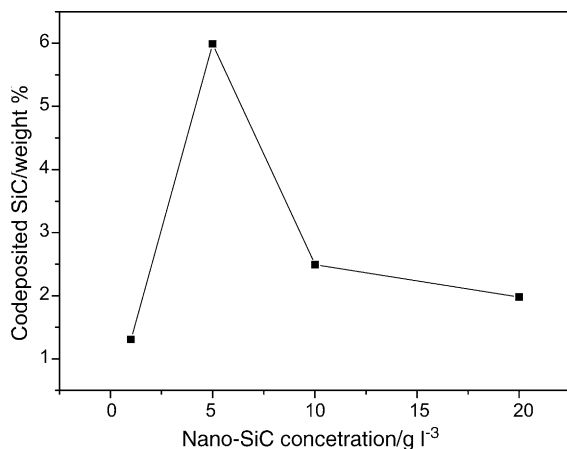


Fig. 3. Weight percentage of co-deposited SiC particulates vs. the concentration of the SiC nano-particulates in the electrolyte ($j_k = 20 \text{ mA cm}^{-2}$, 120 rpm, $T = 40 \text{ }^\circ\text{C}$).

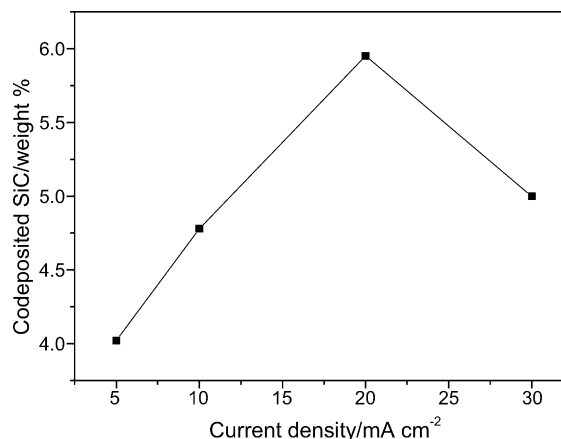


Fig. 4. Weight percentage of co-deposited SiC particulates vs. the current density (5 g L^{-1} SiC, 120 rpm, $T = 40 \text{ }^\circ\text{C}$).

of the SiC particulates in the electrolyte owing to their poor wettability.

Fig. 4 shows the effect of current density on the content of the co-deposited SiC from a bath containing 5 g L^{-1} of SiC particles at 120 rpm and $40 \text{ }^\circ\text{C}$. It is observed that the content of the co-deposited SiC nano-particulates increases initially with the current density and reaches a maximum at 20 mA cm^{-2} . Beyond this current density, the weight percentage of the co-deposited SiC particulates decreases. This result is in agreement with earlier observations by Wu et al. for Co–Ni– Al_2O_3 [18], Muller et al. for ZnNi/SiC [19], and Wang et al. for Al_2O_3 –Cu (Sn) systems [22]. Before the maximum the increasing content of SiC can be attributed to the increasing tendency for absorbed particles to arrive in the cathode surface, which is consistent with Guglielmi's model [21]. The process is controlled by the adsorption of the particles and the particle deposition is dominant. When current density is greater than 20 mA cm^{-2} , the decreasing trend can be explained by the fact that an increase in current density results in more rapid deposition of the metal matrix and fewer particles are embedded in the coating. Hence, the metal deposition dominates the co-deposition process.

The stirring rate strongly affects the weight percentage of the co-deposited SiC particulates since SiC should be transported to the cathode surface for the co-deposition. The influence of stirring rate on the weight percentage of the co-deposited SiC particulates is shown in Fig. 5. The weight percentage increases

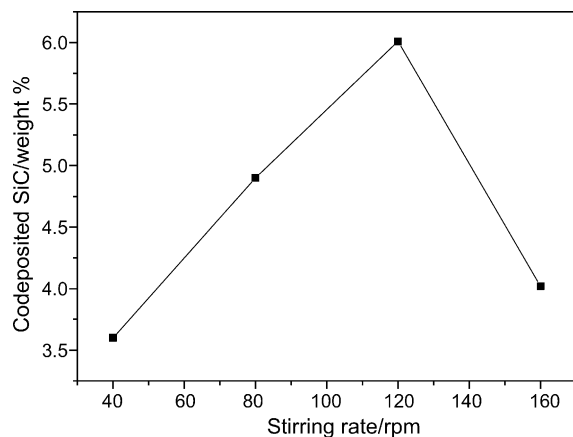


Fig. 5. Weight percentage of co-deposited SiC particulates vs. the stirring rate (5 g L^{-1} SiC, $j_k = 20 \text{ mA cm}^{-2}$, $T = 40^\circ \text{C}$).

with stirring rate and reaches a maximum value at 120 rpm, then decreases with increasing the stirring rate. When the stirring rate is lower than 120 rpm, the fluid flow is not capable of transporting all the particulates to the cathode surface and the co-deposition behavior of SiC particulates is apparently controlled by particulate transfer. When the stirring rate is too high, the decreasing trend of the weight percentage is principally caused by the collision factor [23]. Another reason is perhaps that the increasing streaming velocity of the suspension may also sweep away the loosely adsorbed SiC particulates on the cathode surface, and make the rate of particulates removal higher than that of attachment, resulting in a decrease in the weight percentage of the co-deposited SiC nano-particulates in the composite coating.

Fig. 6 shows the variation of the weight percentage of the co-deposited SiC with the temperature of the plating bath. It is seen that the weight percentage of the co-deposited SiC increases with the plating bath temperature up to 40°C . Below 40°C , the activity of the particulates increases with increasing plating bath temperature, which is beneficial for the co-deposition of the SiC nano-particulates. However, as the plating bath temperature is higher than 40°C , the thermodynamic movement of the ions is greatly enhanced, which results in the increase of the kinetic energy of the SiC nano-particulates. A similar result is observed by Kim and Yoo [24]. According to Langmuir adsorption theory, the increase in temperature leads to the decrease in the adsorbability of the particulates

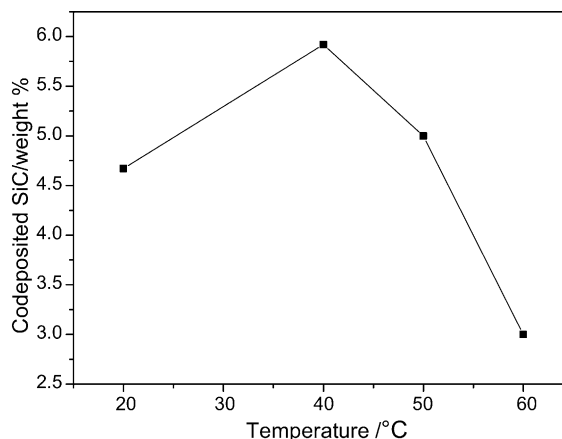


Fig. 6. Weight percentage of co-deposited SiC particulates vs. the temperature of the bath (5 g L^{-1} SiC, 120 rpm, $j_k = 20 \text{ mA cm}^{-2}$).

and hence to decrease the overpotential of the cathode and the electric field, which makes it harder for the SiC particulates to be embedded in the coating matrix and subsequently leads to a decrease in the weight percentage of the co-deposited SiC nano-particulates in the composite coating.

3.4. Surface morphology and structure of the nanocomposite coating

Fig. 7 shows the XRD patterns of the electrodeposited Ni–Co and Ni–Co/2.59% SiC nanocomposite coatings. The XRD pattern confirms that the electrodeposited Ni–Co alloy coating is composed of a solid solution (see Fig. 7a). The intensity of the diffraction peaks of the Ni–Co in the nanocomposite coating is lower and the peak width is broader than that of the Ni–Co alloy coating (see Fig. 7b). This is attributed to the decrease in the grain size of the Ni–Co/SiC nanocomposite coating by the addition of SiC nano-particulates into the plating bath. Namely, the growth of the electrodeposited layer is a competition between the nucleation and crystal growth. SiC nano-particulates provide more nucleation sites and hence retard the crystal growth; subsequently the corresponding Ni–Co matrix in the composite coating has a smaller crystal size.

Fig. 8 shows the SEM morphologies of the Ni–Co alloy coating and Ni–Co/SiC nanocomposite coating electrodeposited from the electrolyte solution containing 4.68% nano-sized SiC. It is seen that the Ni–Co

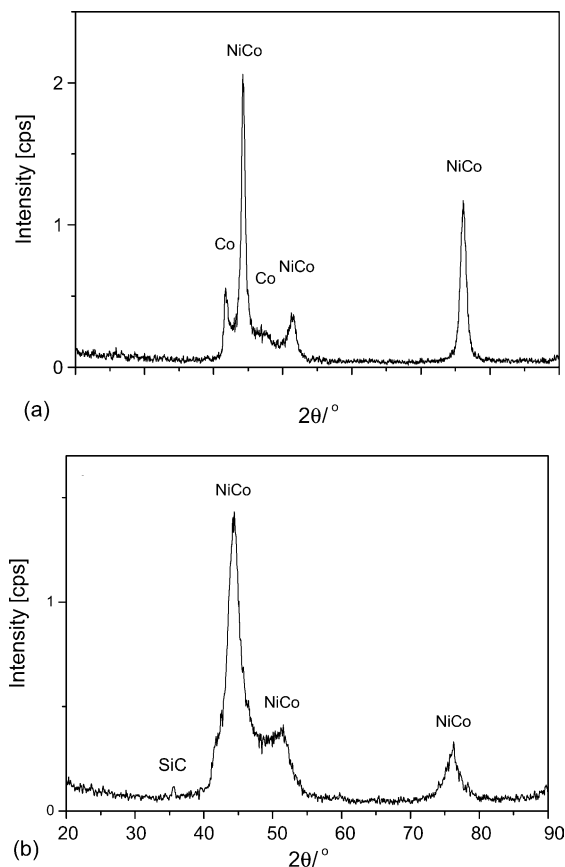


Fig. 7. XRD patterns of (a) Ni–Co alloy without SiC and (b) Ni–Co/SiC nanocomposite coating obtained from bath containing 2.59% SiC.

alloy coating is characterized by needle-like microcrystallite structure (see Fig. 8a). Different from the Ni–Co alloy coating, the Ni–Co/SiC nanocomposite coating is characterized by particulate-like structure (see Fig. 8b), which indicates that the co-deposited SiC nano-particulates are much uniformly distributed in the Ni–Co matrix of the nanocomposite coating. In addition, many nodular agglomerated grains are seen on the nanocomposite coating surface (Fig. 8c). It is supposed that the co-deposited SiC nano-particulates of a uniform distribution and agglomeration to some extent may contribute to increasing the wear resistance of the Ni–Co/SiC nanocomposite coating. The cross-section SEM image of the nanocomposite coating has been shown in Fig. 9. It shows that Ni–Co/SiC nanocomposite coating is fairly uniform, continuous and compact.

3.5. Microhardness and friction and wear behavior of the nanocomposite coatings

Fig. 10 shows the variation in the microhardness and wear rate of the Ni–Co/SiC nanocomposite coatings with the content of nano-SiC. It is seen that the Ni–Co/4.68% SiC nanocomposite coating has a maximum hardness and minimum wear rate, which is in accordance with Archard's law [25]. The microhardness of the nanocomposite coatings increases with increasing weight percentage of the nano-SiC, similar to what has been reported on Ni/Si₃N₄ [9], Ni/TiO₂ [23], and Ni/WC composite coatings [27]. The increase in the microhardness and the decrease in the wear rate of the Ni–Co/SiC nanocomposite coatings as compared to the Ni–Co coating is rationally understood, since the SiC nano-particulates co-deposited in the Ni–Co alloy matrix could restrain the growth of the Ni–Co alloy grains and the plastic deformation of the matrix under a loading, by way of grain-finishing and dispersive strengthening effects. The grain-finishing and dispersive strengthening effects become stronger with increasing nano-SiC content, thus the microhardness and wear resistance of the Ni–Co/SiC composite coatings increase with increasing nano-SiC content.

Fig. 11 shows the Tafel curves measured for the Ni–Co alloy coating and Ni–Co/SiC nanocomposite coating in 0.5 mol L⁻¹ NaCl solution. A small current plateau is observed in the Tafel curve of the Ni–Co/3.2% SiC nanocomposite coating, which could be associated with an accelerated passivation process. The corrosion current density values were estimated making use of Tafel slope method [28]. The corrosion potential and corrosion current for the Ni–Co/3.2% SiC nanocomposite coating, obtained from the polarization curves were -0.33 V and 7.9×10^{-3} A/cm², respectively; and those for the Ni–Co alloy coating were determined to be -0.39 V and 3.98×10^{-2} A/cm², respectively. It is seen that the nanocomposite coatings have lower positive corrosion potentials and smaller corrosion current densities than the Ni–Co alloy coating. In other words, the Ni–Co/SiC nanocomposite coatings have better corrosion resistance than the Ni–Co alloy coating; i.e., the Ni–Co/SiC nanocomposite coatings have lower chemical activity than the Ni–Co alloy coating and hence possess better chemical stability in the external

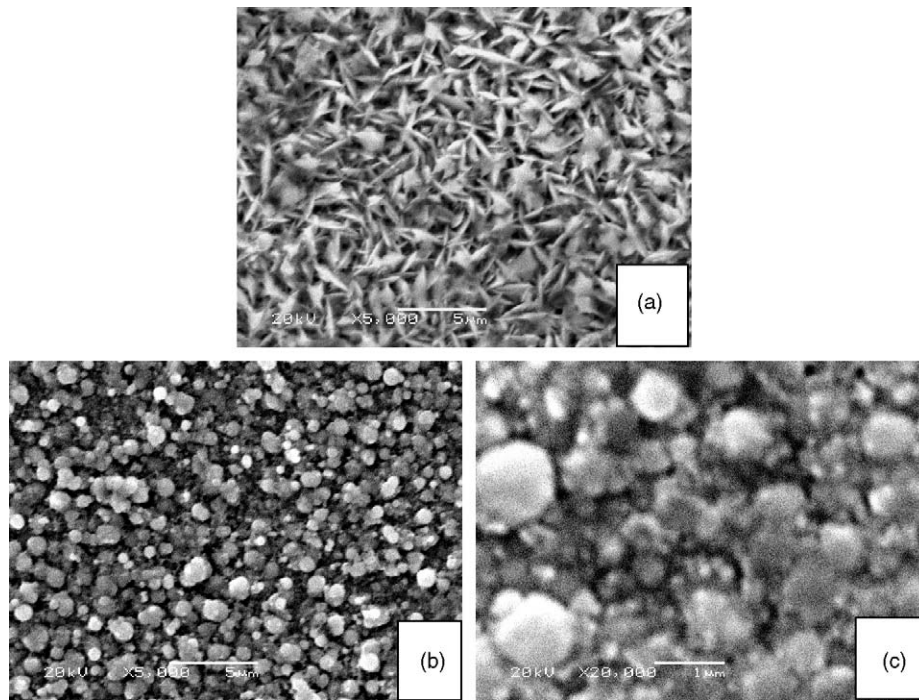


Fig. 8. SEM surface morphology of (a) Ni-Co alloy coating and (b) and (c) Ni-Co/4.68% SiC nanocomposite coating (where (c) is the magnified image of (b)).

environment. This observation is contrary to what has been observed for the corrosion resistance of alumina–nickel composite coating [29] but similar to what have been reported on the corrosion resistance of carborundum–nickel [11] and titania–nickel nanocomposite coatings [26]. The better electrochemical performance

of the Ni-Co/SiC nanocomposite coatings may be attributed to the reduction in the defect size of the nanocomposite coatings by the incorporation of nanoparticles, which is helpful to segregate the corrosive medium. Besides, the deposition of the SiC nano-particulates in the composite coatings can

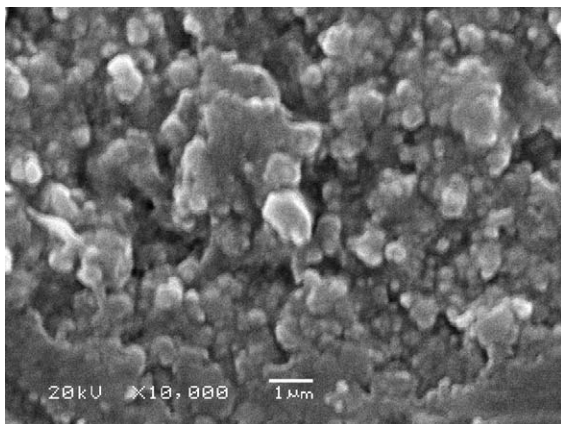


Fig. 9. SEM cross-section image of Ni-Co/4.68% SiC nanocomposite coating.

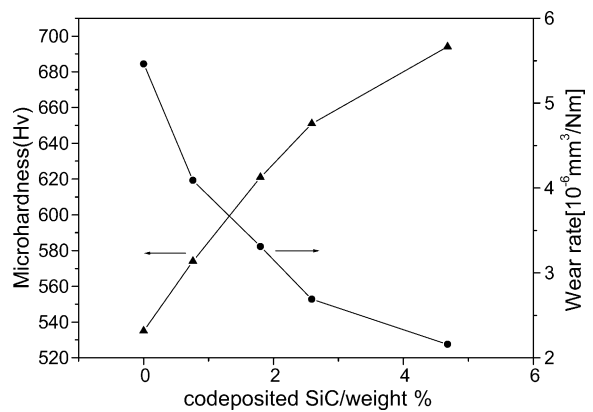


Fig. 10. Microhardness and wear rate of the nanocomposite coatings vs. weight percentage of co-deposited SiC particulates in the nanocomposite coating.

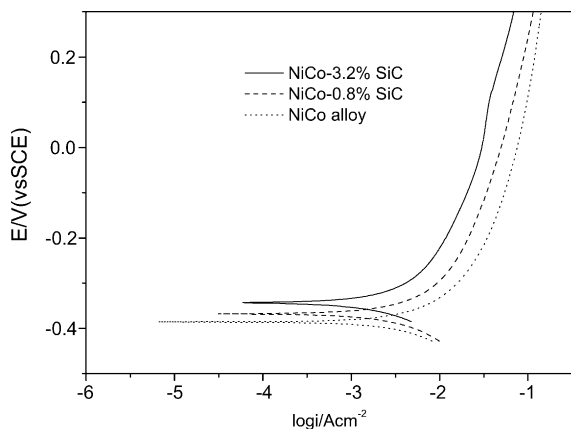


Fig. 11. Tafel curves of Ni–Co alloy coating and Ni–Co/SiC nanocomposite coatings in 0.5 mol L^{-1} NaCl solution.

also help to prevent the corrosive pits from growing up, and the incorporation of nano-particulates contributes to accelerate the passivation process of the metal matrix as well. Subsequently, the corrosion resistance of the nanocomposite coatings was improved.

4. Conclusions

It is feasible to prepare Ni–Co/SiC nanocomposite coating by properly incorporating the nano-particulates to be co-deposited in the Ni–Co plating bath. The cathodic polarization potential of the Ni–Co/SiC electrolyte increases with increasing SiC concentration in the plating bath, but the co-deposited SiC nano-particulates do not significantly affect the electrodeposition process of the Ni–Co alloy coating. It is recommended to prepare the Ni–Co/SiC nano-particulates composite coating of the largest weight percentage of SiC particulates by plating in the bath containing 5 g L^{-1} SiC nano-particulates at a temperature of $40 \text{ }^\circ\text{C}$, current density of 20 mA cm^{-2} , and a stirring rate of 120 rpm. The Ni–Co in the composite coating has a larger peak width than the Ni–Co alloy coating, which is attributed to the decrease in the grain size of the Ni–Co/SiC composite coating by the addition of SiC nano-particulates into the plating bath. The incorporation of the SiC nano-particulates leads to the changes in the morphology, microhardness and wear resistance of the nanocomposite coatings as

compared to the Ni–Co alloy coating. Namely, the Ni–Co/SiC nanocomposite coatings have higher microhardness and better wear resistance than the Ni–Co alloy coating, which is attributed to the grain-finishing and dispersive strengthening effects of the co-deposited hard SiC nano-particulates. The better corrosion resistance of the Ni–Co/SiC nanocomposite coatings may be ascribed to the favorable chemical stability of the SiC nano-particulates, which help to reduce the hole size in the nanocomposite coatings and prevent the corrosive pits from growing up.

Acknowledgements

The work was supported by the National Natural Science Foundation of China (Grant No. 50405040), the Ministry of Science and Technology of China (Grant No. 2002AA302609), and the Innovative Group Foundation from NSFC (Grant No. 50421502). The authors thank Prof. J.Z. Zhao and Mr. D.K. Song for their help in the SEM, EDS, and XRD measurements.

References

- [1] P.A. Gay, P. Berçot, J. Pagetti, *Surf. Coat. Technol.* 140 (2001) 147.
- [2] A. Grosjean, M. Rezzazi, J. Takadoum, P. Berçot, *Surf. Coat. Technol.* 137 (2001) 92.
- [3] A.F. Zimmerman, G. Palumbo, K.T. Aust, U. Erb, *Mater. Sci. Eng. A* 328 (2002) 137.
- [4] K.H. Hou, M.D. Ger, L.M. Wang, S.T. Ke, *Wear* 253 (2002) 994.
- [5] W.X. Chen, J.P. Tu, L.Y. Wang, H.Y. Gan, Z.D. Xu, X.B. Zhang, *Carbon* 41 (2003) 215.
- [6] P.C. Searson, T.P. Moffat, *Crit. Rev. Surf. Chem.* 3 (1994) 171.
- [7] D. Clark, D. Wood, U. Erb, *Nanostruct. Mater.* 9 (1997) 755.
- [8] F. Hu, K.C. Chan, *Appl. Surf. Sci.* 243 (2005) 251.
- [9] C.S. Ramesh, S.K. Seshadri, *Wear* 255 (2003) 893.
- [10] I. Garcia, J. Fransaer, J.P. Celis, *Surf. Coat. Technol.* 148 (2001) 171.
- [11] L. Benea, P.L. Bonora, A. Borello, S. Martelli, *Mater. Corros.* 53 (2002) 23.
- [12] L.P. Wang, Y. Gao, Q.J. Xue, H.W. Liu, T. Xu, *Appl. Surf. Sci.* 242 (2005) 326.
- [13] N. Fenineche, C. Coddet, A. Saida, *Surf. Coat. Technol.* 41 (1990) 75.
- [14] S.N. Srimathi, S.M. Mayanna, B.S. Sheshadri, *Surf. Technol.* 16 (1982) 277.

- [15] H. Zhu, S.G. Yang, G. Ni, D.L. Yu, Y.W. Du, *Scripta Mater.* 44 (2001) 2291.
- [16] C.A. Moina, M. Vazdar, *Electrochem. Commun.* 3 (2001) 159.
- [17] X.C. Li, Z.W. Li, *Mater. Sci. Eng. A* 358 (2003) 107.
- [18] G. Wu, N. Li, D.R. Zhou, K.C. Mitsuo, *Surf. Coat. Technol.* 176 (2003) 157.
- [19] C. Müller, M. Sarret, M. Benballa, *Surf. Coat. Technol.* 162 (2002) 49.
- [20] S.C. Wang, J. Wei, Wen-Cheng, *Mater. Chem. Phys.* 78 (2003) 574–580.
- [21] N. Guglielmi, *J. Electrochem. Soc.* 119 (8) (1972) 1009.
- [22] Y.L. Wang, Y.Z. Wan, Sh. M. Zhao, H.M. Tao, X.H. Dong, *Surf. Coat. Technol.* 106 (1998) 162.
- [23] S.H. Yeh, C.C. Wan, *Plat. Surf. Finish.* 84 (1997) 54.
- [24] S.K. Kim, H.J. Yoo, *Surf. Coat. Technol.* 108/109 (1998) 564–56.
- [25] D.H. Jeong, F. Gonzalez, G. Palumbo, et al. *Scripta Mater.* 44 (2001) 493.
- [26] J. Li, Y. Sun, X. Sun, J. Qiao, *Surf. Coat. Technol.* 192 (2004) 331.
- [27] M. Surender, B. Basu, R. Balasubramaniam, *Tribol. Int.* 37 (2004) 743.
- [28] C.M.A. Brett, A.M. Oliveira Brett, *Electrochemistry: Principles, Methods and Applications*, Oxford University Press, 1998.
- [29] F. Erler, C. Jakob, H. Romanus, L. Spiess, B. Wielage, T. Lampke, S. Steinhouser, *Electrochim. Acta* 48 (2003) 3063.